Optical clumped isotope thermometry of carbon dioxide

Ivan Prokhorov, Tobias Kluge, Christof Janssen

SCIENTIFIC REPORTS

OPEN

Optical clumped isotope thermometry of carbon dioxide

Ivan Prokhorov[1,2,3], Tobias Kluge[1,2] & Christof Janssen[1,3]

Received: 4 September 2018
Accepted: 22 February 2019
Published online: 18 March 2019

Simultaneous analysis of carbon dioxide isotopologues involved in the isotope exchange between the doubly substituted $^{13}C^{16}O^{18}O$ molecule and $^{12}C^{16}O_2$ has become an exciting new tool for geochemical, atmospheric and paleoclimatic research with applications ranging from stratospheric chemistry to carbonate-based geothermometry studies. Full exploitation of this isotope proxy and thermometer is limited due to time consuming and costly analysis using mass spectrometric instrumentation. Here, we present an all optical clumped CO_2 isotopologue thermometer with capability for rapid analysis and simplified sample preparation. The current development also provides the option for analysis of additional multiply-substituted isotopologues, such as $^{12}C^{18}O_2$. Since the instrument unambiguously measures all isotopologues of the $^{12}C^{16}O_2 + {}^{13}C^{16}O^{18}O \rightleftharpoons {}^{13}C^{16}O_2 + {}^{12}C^{16}O^{18}O$ exchange, its equilibrium constant and the corresponding temperature are measured directly. Being essentially independent of the isotope composition of the calibration gas, an uncalibrated working reference is sufficient and usage of international calibration standards is obsolete. Other isotopologues and molecules can be accessed using the methodology, opening up new avenues in isotope research. Here we demonstrate the high-precision performance of the instrument with first gas temperature measurements of carbon dioxide samples from geothermal sources.

Mass spectrometry of multiply substituted isotopologues or clumped isotopes has become an extremely powerful tool in the natural sciences. Demonstrated applications which investigated carbon dioxide, methane, nitrous oxide, molecular hydrogen and oxygen range from tectonic history and evolution, geobiology and atmospheric chemistry over the investigation of non-equilibrium processes with correction procedures, diagenesis studies, the investigation of mineral formation conditions, the assessment of hydrothermal flow systems and paleo-evolution to paleothermometry; and there are many more potential applications[1,2]. The most prominent uses are linked to the oxygen isotope exchange reaction between the main isotopologue and the ^{13}C-^{18}O containing species of CO_2

$$^{12}C^{16}O_2 + {}^{13}C^{16}O^{18}O \rightleftharpoons {}^{13}C^{16}O_2 + {}^{12}C^{16}O^{18}O. \quad \text{(R1)}$$

Reaction (R1) involves only a single chemical compound, but could not be exploited scientifically until recently. This is because their very low natural abundance hampers the study of multi-substituted isotopic molecules, such as $^{13}C^{16}O^{18}O$, containing two or more rare isotopes (e.g. ^{13}C and ^{18}O) simultaneously. When compared to the main isotopologue $^{12}C^{16}O_2$, these are well below 10^{-4} (see Table 1). At the same time, the measurement techniques needed to attain extremely high accuracy levels of a few 0.01‰ (~tens of ppm) in order to trace the natural variability of the corresponding isotopologue and a dynamic range on the order of about 10^9 or better is therefore required. So far, only mass spectrometer instruments are capable of fulfilling these criteria and clumped CO_2 has not yet been measured by optical methods[1,2]. Doubly substituted $^{13}CH_3D$ methane, which shows higher fractionation values, however, has been investigated using laser-based instruments. The first laser spectrometer setup[3] for clumped methane isotopologues based on difference frequency generation (DFG) still suffered from uncertainties in the 20‰ range which exceeds natural $^{13}CH_3D$ variability of about 8‰[4]. Nevertheless, a more recent diode laser study on doubly substituted methane[5] has successfully demonstrated that optical systems can well approach the necessary requirements. The achieved precision level of 200 ppm, however, remains still well above the commonly accepted threshold of 100 ppm (or 0.1‰) required for the study of clumped isotope fractionation in non-hydrogenated molecules.

[1]Institute of Environmental Physics, Heidelberg University, 69120, Heidelberg, Germany. [2]Heidelberg Graduate School of Fundamental Physics, Heidelberg University, 69120, Heidelberg, Germany. [3]LERMA-IPSL, Sorbonne Université, CNRS, Observatoire de Paris, PSL Université, 75005, Paris, France. Correspondence and requests for materials should be addressed to C.J. (email: christof.janssen@obspm.fr)

Isotopologue i		Mass (u)[a]	Rel. abundance $n_i/\Sigma_j n_j$ (mol/mol)	Rel. contribution to mass (%)	Note
No	Symbol				
1	$^{12}C^{16}O_2$	44	$9.842 \cdot 10^{-1}$	100.000	
2	$^{13}C^{16}O_2$	45	$1.100 \cdot 10^{-2}$	93.636	
3	$^{12}C^{16}O^{18}O$	46	$3.947 \cdot 10^{-3}$	99.785	
4	$^{12}C^{16}O^{17}O$	45	$7.478 \cdot 10^{-4}$	6.364	b
5	$^{13}C^{16}O^{18}O$	47	$4.413 \cdot 10^{-5}$	96.710	
6	$^{13}C^{16}O^{17}O$	46	$8.361 \cdot 10^{-6}$	0.211	
7	$^{12}C^{18}O_2$	48	$3.957 \cdot 10^{-6}$	99.578	c
8	$^{12}C^{17}O^{18}O$	47	$1.500 \cdot 10^{-6}$	3.286	
9	$^{12}C^{17}O_2$	46	$1.421 \cdot 10^{-7}$	0.004	
10	$^{13}C^{18}O_2$	49	$4.424 \cdot 10^{-8}$	100.000	
11	$^{13}C^{17}O^{18}O$	48	$1.676 \cdot 10^{-8}$	0.422	
12	$^{13}C^{17}O_2$	47	$1.588 \cdot 10^{-9}$	0.003	

Table 1. Typical relative abundance of stable CO_2 isotopologues in decreasing order. Abundance values are based on assuming a statistical distribution of oxygen and carbon isotopes in international standard materials (VSMOW for O and VPDB for C: $^{13}R = 11056/988944$, $^{17}R = 3790/9976206$, $^{18}R = 20004/9976206$)[53]. [a]Atomic mass constant. [b]Can only be measured after conversion[10,11] into O_2 or using isotope exchange techniques[12]. [c]Signal used to detect contaminant species, such as hydrocarbons or halogenated compounds[14].

While mass spectrometers excel in the achieved precision of about 10 to 20 ppm[6,7], the instruments have to cope with inherent drawbacks. Not only are they relatively costly and heavy, thus not permitting in-field operation; they also require time consuming measurements and careful sample preparation in order to avoid contamination of the measurement signal. With current mass spectrometric procedures, preparation and analysis of a carbonate sample take about 3 to 6 h[8]. Importantly, only the largest and most sophisticated instruments can reach the mass resolution required to resolve isobaric interferences in CO_2[9]. Typical operation conditions are around $\Delta M/M \sim 40000$ or lower, which is insufficient to separate $^{13}C^{16}O_2$ from $^{12}C^{16}O^{17}O$ at m/z = 45 or $^{13}C^{16}O^{18}O$ from $^{12}C^{17}O^{18}O$ at m/z = 47, for example. In order to resolve these masses, a resolving power of above 52000 is needed – so far only accessible for large radius instruments in 'non-normal operation' mode[9]. This makes multiply substituted isotopologue analysis by mass spectrometry a very exclusive technology that will remain limited to only a handful of highly specialised laboratories worldwide, likely also constraining industrial or commercial use. Note that only two ($^{12}C^{16}O_2$ and $^{13}C^{18}O_2$) out of twelve stable CO_2 isotopologues can be detected entirely free from isobaric interference using a mass spectrometer (see Table 1). The four isotopologues $^{13}C^{16}O_2$, $^{12}C^{16}O^{18}O$, $^{13}C^{16}O^{18}O$, and $^{12}C^{18}O_2$, strongly dominate (>90%) a cardinal mass signal. They can thus well be assessed by the same technology except $^{12}C^{18}O_2$, whose quantification suffers from distorting background signals. For minor contributions to a cardinal mass, such as $^{12}C^{16}O^{17}O$ however, more advanced sample preparation or conversion technologies[10–12] must be employed at the cost of prolonged measurement time and reduced precision.

Simple counting statistics prevent using current mass spectrometer technology for the analysis of CO_2 isotopologues below the relative abundance level of 10^{-5}, even if these provide the main contribution to a cardinal mass. Assuming the measurement uncertainty being limited by Poisson statistics, the 10 ppm precision is reached after about 3 or 4 h of measurement on m/z = 47 ($^{13}C^{16}O^{18}O$)[13]. In order to obtain the same precision for the $^{12}C^{18}O_2$ isotopologue on m/z = 48, a $(n(^{16\ 13}C^{16}O^{18}O)/n(^{12}C^{18}O_2))^2 \sim 100$ times longer analysis time would be required, thus about two weeks. Even measurement times of two days are impractical and contrary to common practice. Demonstrations of ppm level instrument stabilities over such long time periods are lacking too. The m/z = 48 and 49 signals can therefore only be used as an indicator for sample contamination (hydrocarbons, halocarbons, sulphur monoxide)[1,14,15] and must remain useless in exploiting $^{12}C^{18}O_2$ or $^{13}C^{18}O_2$ as isotopic tracers with mass spectrometry.

Despite the pioneering achievements of mass spectrometry in rare multi-isotope research, it is evident that alternative technologies are needed to overcome several of the aforementioned limitations. In this paper, we will present the first optical multi-isotopologue analyser for CO_2 that is not influenced by most of these limitations, most notably the isobaric interference problem. The instrument achieves a measurement accuracy well below the 100 ppm level in the measurement of $^{13}C^{16}O^{18}O$ and the technique has the capacity of assessing new tracers such as $^{12}C^{18}O_2$ that likely provide new and complementary information. In principle the developed method is calibration free and has strong potential of becoming a breakthrough technology, because it provides great isotopologue selectivity at reduced time, size and cost factors, which makes it well suited for widespread scientific, laboratory and commercial applications. The paper focusses on the measurement of carbon dioxide and the isotope exchange in the gas phase and we present the analysis of CO_2 from thermal sources in the Upper Rhine Valley. The results will be compared to duplicate mass spectrometer measurements of CO_2 from the same source. Apart from direct studies of gaseous carbon dioxide, current applications are concerned with multiply-substituted isotopologues in carbonates. Because carbonate isotopologues are obtained from measurements of gaseous CO_2 released during the acid digestion of the carbonates, they can be investigated using the same analysis systems. The direct application of carbon dioxide isotopologue analysis to carbonates is further facilitated by the fact that the carbonate clumped isotope scale has been directly tied into the equilibrium CO_2 gas scale[6].

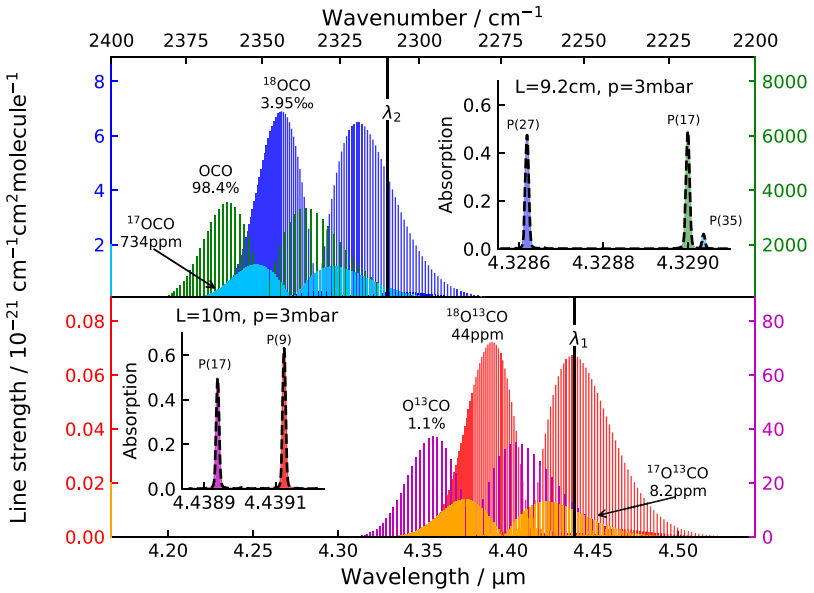

Figure 1. Mid-infrared spectra of CO_2 isotopologues. The top panel shows spectra around the 4.33 µm laser wavelength for the detection of the main isotopologue ($^{12}C^{16}O_2$), and the two singly substituted oxygen species $^{12}C^{16}O^{17}O$ and $^{12}C^{16}O^{18}O$. The lower panel displays spectra of ^{13}C containing isotopologues ($^{13}C^{16}O_2$, $^{13}C^{16}O^{17}O$, and $^{13}C^{16}O^{18}O$) at 4.44 µm. Broadband spectra in main panels were simulated using the HITRAN[41] database. The insets zoom in on the measured absorption of selected lines at corresponding path lengths and the typical sample pressure of 3 mbar. Black dashed lines represent the experimentally measured spectra and shaded areas the fit of the respective isotopologue line area.

Operating Principles and Instrumental Approach

Isotopologue absorption spectroscopy. The optical measurement of CO_2 isotopologues is based on absorption of isotopologue dependent ro-vibrational transitions in the ν_3 fundamental band around 4 µm (Fig. 1), where infra-red absorption of carbon dioxide is strongest. With respect to the ^{12}C containing species, the vibrational bands of ^{13}C containing isotopologues are shifted towards lower energies. Using simultaneously two tuneable inter-band cascade lasers (ICLs) at 4.3 and 4.4 µm and absorption-balanced light paths of 9.2 cm and 10 m length, respectively, absorption signals of several ten percent of the five most abundant isotopologues can be obtained when a few mbar of pure CO_2 are analysed in a cylindrical 0.8 L thermostated stainless steel absorption cell. A Herriott cell configuration made out of two concave mirrors at a distance of about 17.6 cm has been realised in order to achieve the long light path with 58 reflections. The short path traverses the cell just once in the perpendicular direction. More information on the absorption lines and a more detailed description of the set up displayed in Fig. 2 are given elsewhere[16].

Spectra of pure CO_2 at 297 K and 3 to 4 mbar are recorded at a rate of 1.56 kHz by driving laser currents at the same pace. A non-linear current ramp has been chosen for minimising the non-linearity of the laser frequency response over time[17]. Individual spectra were then averaged over 1 s time interval and analysed using a home-built fitting routine employing Rautian line profiles[18]. Required line parameters have been taken either from the HITRAN database (position) or were determined in separate experiments (self broadening coefficient and frequency of velocity changing collisions)[16]. The particle number density n of an isotopologue is obtained from applying the Beer-Lambert law to one of its transitions (see insets in Fig. 1), located at the centre wavenumber $\nu = \nu_c$. For a spectrally narrow laser the CO_2 gas number density ($n(CO_2) = [CO_2]$) is linked to the optical measurement via[19]

$$[CO_2] = -\frac{\ln(Tr(\nu))}{S \cdot g(\nu - \nu_c) \cdot L} = \frac{\alpha}{\sigma \cdot L}, \tag{1}$$

where L is the path length, $Tr(\nu)$ the transmittance, S the line strength and $g(\nu - \nu_c)$ the molecular line shape function of the particular transition. Isotopologue concentrations can thus be obtained from the extinction coefficient $\alpha = -\ln(Tr(\nu_c))$ and the absorption cross section $\sigma = S \cdot g(0)$ at peak centre, which remain constant under fixed experimental conditions. The path length cancels in the measurement of an isotopologue ratio when both isotopologues are detected using the same path, e.g.[20]. $[CO_2]_1/[CO_2]_2 = \alpha_1/\alpha_2 \cdot (\sigma_1/\sigma_2)^{-1}$, making the method immune against eventual slight path length changes. Note that in spite of using the simplifying notation on the right hand side of Eq. (1) spectra are fitted over a whole frequency window and therefore include information from entire absorption lines and not just from peak absorption values.

Duplicate isotope ratio mass spectrometer (IRMS) measurements have been performed using the ThermoFischer MAT253Plus instrument at IUP Heidelberg, that has been equipped with an additional m/z = 47.5

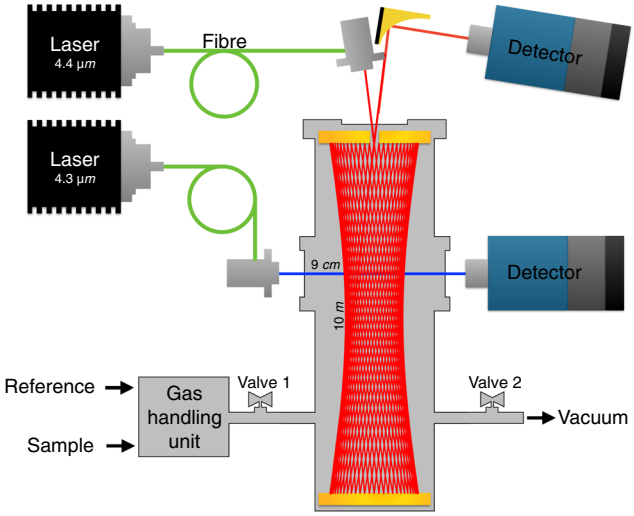

Figure 2. Scheme of the dual-laser system. Lasers are connected to the absorption cell via optical fibres. An off-axis parabolic mirror focusses the exiting light from the multi-pass cell on a photo-detector. The light of the single pass is projected on a second detector without further focussing. The cell is filled with sample and reference gases via a custom-built inlet system and can be evacuated using a second gas connection.

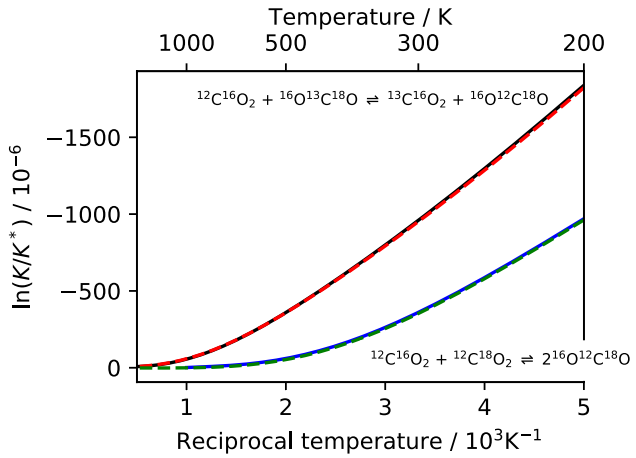

Figure 3. Isotope equilibria of the $^{12}C^{16}O_2 + {}^{13}C^{16}O^{18}O$ (R1) and the $^{12}C^{18}O_2 + {}^{12}C^{16}O_2$ (R2) exchange reaction at temperatures between 200 and 1500 K. The logarithm of the normalised equilibrium constants K/K^* is shown, where $K_1^* = 1$ and $K_2^* = 4$ are the statistical (high temperature) limits. Statistical mechanics calculations[22] from partition function ratios according to Bigeleisen-Mayer-Urey (BMU, hereafter) theory[25] (red and green dashes) and direct sum calculations (black and blue lines) based on new spectroscopic data generated from experimentally refined ab initio calculations[34] are displayed.

cup and 10^{13} Ω resistors on m/z = 47−49 mass cups[16]. The m/z = 47.5 is used for continuous baseline monitoring. The mass spectrometric analysis follows accepted procedures[6,14], as does the sample processing and cleaning[8].

Equilibrium constant, thermodynamics and Δ_{47}. The equilibrium constant K_1 of the isotope exchange reaction (R1) is strictly proportional to the product of absorption signals $A = \alpha_{^{13}C^{16}O_2}\,\alpha_{^{12}C^{16}O^{18}O}\,\alpha^{-1}_{^{12}C^{16}O_2}\,\alpha^{-1}_{^{13}C^{16}O^{18}O}$, which therefore allows for the optical measurement via

$$K_1 = \frac{[^{13}C^{16}O_2][^{12}C^{16}O^{18}O]}{[^{12}C^{16}O_2][^{13}C^{16}O^{18}O]} = \Sigma \times A, \tag{2}$$

where the scaling factor $\Sigma = \sigma_{^{12}C^{16}O_2}\,\sigma_{^{13}C^{16}O^{18}O}\,\sigma^{-1}_{^{13}C^{16}O_2}\,\sigma^{-1}_{^{12}C^{16}O^{18}O}$ depends on the involved molecular line strengths. Lacking the required accuracy, current database values cannot be used for determining Σ, which best is determined experimentally by exploiting the temperature dependence of K_1 or its logarithm (see Fig. 3). The latter is widely used, because deviations from the statistical value ($K_1^* = 1$, where the *-symbol indicates the high temperature limit) are small and it can be expressed by three individual logarithmic terms, which can be

identified with the isotopologue specific enrichment or fractionation values (CO_2 denoting any particular isotopologue in the following equation)

$$\Delta(CO_2) = \frac{[CO_2]}{[CO_2]^*} / \frac{[^{12}C^{16}O_2]}{[^{12}C^{16}O_2]^*} - 1 \simeq \ln(1 + \Delta(CO_2)), \tag{3}$$

commonly used for the quantification of isotopomers[21] or multiply substituted isotopologues[22,23]:

$$-\ln\left(\frac{K_1}{K_1^*}\right) = \ln\left(\frac{[^{13}C^{16}O^{18}O]}{[^{13}C^{16}O_2]}\frac{[^{12}C^{16}O_2]}{[^{12}C^{16}O^{18}O]}\right) = \ln\left(\frac{[^{13}C^{16}O^{18}O]}{[^{13}C^{16}O_2]}\right) - \ln\left(\frac{[^{12}C^{16}O^{18}O]}{[^{12}C^{16}O_2]}\right). \tag{4}$$

The right hand side expression is applicable to the optical measurement, which provides the two particular isotopologue ratios as independent observables. As evident from Eq. (4), the temperature information contained in the equilibrium constant does only depend on two concentration ratios, that may be regrouped differently. ln (K_1) is completely independent of the bulk isotope composition. Consequently, the ^{17}O isotopic composition does not at all affect the determination of the equilibrium constant. Bulk isotopic compositions are only introduced when isotopologue concentrations are replaced by Δ values as defined in Eq. (3). Using $K_1^* = 1 = [^{12}C^{16}O^{18}O]^*[^{13}C^{16}O_2]^*/([^{12}C^{16}O_2]^*[^{13}C^{16}O^{18}O]^*)$ and keeping only the leading terms in the Taylor series expansion on both sides, one obtains

$$\frac{K_1}{K_1^*} - 1 \simeq \Delta(^{13}C^{16}O^{18}O) - \Delta(^{13}C^{16}O_2) - \Delta(^{12}C^{16}O^{18}O), \tag{5}$$

where the $\simeq$ sign indicates the approximative character of the relation. This equation, which may also be derived directly from Eq. (24) of Wang *et al.*[22], is very similar to the commonly used definition of Δ_{47} in clumped isotope mass spectrometry of CO_2 [14,24],

$$\Delta_{47} = \Delta(^{47}CO_2) - \Delta(^{46}CO_2) - \Delta(^{45}CO_2), \tag{6}$$

where isotopologues are replaced by m/z signals, because they cannot be measured individually. Comparison of Eqs (5) and (6) leads to the identification of $\Delta_{47} \simeq K_1/K_1^* - 1$ with the relative deviation of the equilibrium constant K_1 from its statistical value. It has been argued that the last two terms on the right hand side are zero[24], but this premise is not completely consistent with the definition of Δ in Eq. (3) and thermodynamic calculations[22] that respectively yield −4 and −11 ppm for $\Delta(^{45}CO_2)$ and $\Delta(^{46}CO_2)$ for CO_2 equilibrated at 300 K. The reason for the conflicting results is that in the one case approximate but precisely measurable and in the other case exact but only approximatively accessible atomic isotope ratios are used in the calculations of the statistical abundances. Nonetheless, the so defined Δ_{47} is overwhelmingly influenced by the first of the three terms, which in turn is to a large extent (97%, see Table 1) dominated by the $^{13}C^{16}O^{18}O$ isotopologue.

Unlike the direct measurement of ln (K_1) according to Eq. (4), mass spectrometer determinations of Δ_{47} not only require measurement of heavy isotopologue abundances. The 'absolute' or bulk isotope composition must also be known in order to determine the statistical abundance of the m/z = 47 signal. This implies determining atomic $^{13}C/^{12}C$, $^{18}O/^{16}O$ or $^{17}O/^{16}O$ ratios (traditionally quantified in terms of $\delta^{13}C$, $\delta^{18}O$ and $\delta^{17}O$ values), necessitating that international standard substances are used and that assumptions on the ^{17}O isotope content are made. In this way systematic biases of up to 40 ppm are introduced[24]. Equally important, mass spectrometers can only approximately access the clumped $^{13}C^{16}O^{18}O$ isotopologue (also due to an ion-source dependent scrambling effect) using the m/z = 47 signal and a corresponding scaling factor must be applied[1,14].

Using the equilibrium constant of an isotope exchange (or isomerisation) reaction with a particular working gas as a thermometer, temperature is directly measured as a thermodynamic variable. The equilibrium constant of an isotope exchange reaction is linked to the reaction free enthalpy ΔF of that reaction $K = \exp(-\Delta F/(kT))$ [25–27], where k is the Boltzmann constant and where we have adopted a per molecule rather than a per mole definition of energies. The free energy of the gas is linked to the gas' molecular partition function, which sums over all energy states ε_i taking degeneracies d_i into account and counting internal energy states from the lowest or zero-point energy (ZPE) ε_0 state of the molecule

$$Q = \sum_i^{levels} d_i e^{-\frac{\varepsilon_i}{kT}} = Q_{trans} Q_{int} e^{-\frac{\varepsilon_0}{kT}}. \tag{7}$$

In the Eq. (7) we have made the usual separation of the centre of mass motion (*trans*) from the molecular internal degrees of freedom (*int*). Since the equilibrium constant is given as a product of partition functions of reactant (*react*) and product (*prod*) molecules[26,27]

$$K = \frac{\prod Q_{prod}}{\prod Q_{react}} = \left(\frac{\prod M_{prod}}{\prod M_{react}}\right)^{3/2} \frac{\prod Q_{int,prod}}{\prod Q_{int,react}} \exp\left(-\frac{\sum \varepsilon_{0,prod} - \sum \varepsilon_{0,react}}{kT}\right), \tag{8}$$

it is amenable to quantum statistical mechanics and computational chemistry methods. Here we have followed the usual simplification to evaluate the ratio of translational partition functions to ratios of molecular masses M[26]. The only non-trivial factors are the total internal partition functions that need to be evaluated separately. If one is mainly interested in isotope fractionation effects, it is convenient to normalise the equilibrium constant by dividing through its classical high temperature limiting value K^*, which is given as the product of the classical symmetry numbers of product and reactant molecules:

$$\frac{K}{K^*} = K\frac{\prod \sigma_{react}}{\prod \sigma_{prod}}.$$

Solving for $\Delta\varepsilon_0 = \sum \varepsilon_{0,prod} - \sum \varepsilon_{0,react}$, one obtains the ZPE change of the reaction in terms of measurable quantities:

$$\Delta\varepsilon_0 = -kT\left[\ln K - \frac{3}{2}\ln\left(\frac{\prod M_{prod}}{\prod M_{react}}\right) - \ln\left(\frac{\prod Q_{int,prod}}{\prod Q_{int,react}}\right)\right]. \quad (9)$$

The different terms in Eq. (9) can be identified with the reaction enthalpy or energy $\Delta H = \Delta U = \Delta\varepsilon_0$, the reaction free enthalpy ($\Delta F = -kT\ln K$), and the free enthalpy change associated to the reaction entropy ($T\Delta S$), which is given by the two remaining terms on the right hand side. Eq. (9) takes into account the energy change associated with the translational and internal molecular motion. In the following we adopt spectroscopic conventions and use term energies in wavenumber units $\Delta\nu = \Delta\varepsilon/hc$, where h and c are the Planck constant and the speed of light, respectively. Different methods have been proposed to calculate the internal partition functions in Eq. (7). The traditional method based on work of Urey, Bigeleisen and Goeppert-Mayer (BMU)[25–27] is to consider molecules as rigid rotor – harmonic oscillators and use corresponding spectroscopic constants. Combination of this approach with the Teller-Redlich rule[28], usually attributed to Urey[29], leads to a very simple description. For better accuracy, anharmonic corrections to vibrational energies and rotation-vibration interactions can be taken into account[25,30,31], but for reasons of convenience or lack of parameters mostly only the anharmonic corrections to the ZPE are applied[22,29]. This can lead to significant uncertainties and more elaborate methods have been proposed, such as calculating the direct sum as a path integral using Monte-Carlo (PIMC) methods[32,33]. If highly accurate potential surfaces with spectroscopic quality are available or global effective Hamiltonians have been determined, such as for CO_2 [34], the total internal partition function in Eq. (7) might also be calculated very accurately by summing directly over all terms. In any case, the standard BMU approach must fail at low temperatures and masses (e.g. H_2) due to neglecting the quantisation of rotational states, which is only taken into account approximately. In such a case the sum in Eq. (7) must be evaluated directly[25]. Conversely, the computational cost associated with numerical methods, such as PIMC and direct summation will increase when the temperature augments, because the number of thermally accessible states increases strongly. In addition the potential energy surface properties far from the equilibrium configuration become important when temperatures raise, leading to numerical convergence problems and artefacts[22,35]. In this limiting case, where isotope fractionation must vanish and a high precision is required, the BMU approach in combination with the Teller-Redlich rule might serve as a particularly useful guide, because its convergence towards the statistical limit is always assured.

Implementation of the spectroscopic measurement. Unlike mass spectrometry, a laser absorption instrument can unambiguously measure all four (or three) required isotopologues of a homogenous CO_2 isotope exchange reaction. The measurement is conceptually straight forward and does not depend on additional determinations and hypotheses on the bulk isotopic composition, as it directly determines $\ln K$ or $\ln(K/K^*)$ and its temperature dependence, disregarding the $\ln\Sigma$ term (see Eqs (2) and (4)), which needs to be determined experimentally using a reference measurement:

$$\ln K_1(T) = \ln A(T) + \ln\Sigma = \ln K_1(T_{ref}) + \ln(A(T)/A_{ref}). \quad (10)$$

Here, $A(T)$ and A_{ref} indicate the measured product of absorbances in Eq. (2) for CO_2, once for the sample and once for a reference gas with known equilibrium constant K_1 that has been equilibrated at the reference temperature T_{ref}. Consequently, the method makes the quantification of the statistical distribution of isotopes obsolete (as indicated by Eq. (4)). Since absolute abundances of C and O isotopes don't need to be known, the absorption measurement dispenses in principle the use and measurement of international standard substances. It only requires the comparison with a working gas whose value of $\ln K$ is known and remains stable over time. The extremely slow gas phase isotope exchange at ambient temperatures assures that any equilibrated CO_2 gas with an isotopic composition close to natural sample gas composition in principle suffices for determining $\ln\Sigma$ (see Eq. (10)). This should make laser-based clumped isotopologue analysis much easier applicable than mass spectrometer investigations. In our setup, however, a slight cross-sensitivity of $\ln K$ on the difference in $\delta^{13}C$ between the sample and the working reference gas of -4 ppm/‰ has been observed. This entails the determination of $\delta^{13}C$ in our samples such that the interference can be corrected empirically[16]. The correction requires only one extra measurement and evaluation step relative to the sophisticated and error-prone mass spectrometric procedure. On the contrary, a cross correlation between $\ln K$ and $\delta^{18}O$ has not been observed. The $\delta^{13}C$ interference is much stronger than the isotope dependence of the thermodynamic equilibrium composition of about -0.01 ppm/‰. The effect is likely due to an insufficient modelling of the baseline originating from strong nearby absorption features of $^{13}CO_2$. An improved fitting algorithm and a better choice of the spectral micro-window for the absorption lines should eliminate the effect, but this hypothesis requires further examination.

A natural candidate for the calibration of the optical method using Eq. (10) are measurements of the equilibrium constant at the high temperature limit ($\ln K_1(T > 2000\ \mathrm{K}) \simeq \ln K_1^* = 0$). As these conditions are difficult to realise experimentally, we use a two step calibration, involving a heated working reference gas at a lower temperature and an ambient temperature working reference gas. The hot CO_2 serves as calibration point, that determines the origin of the optical $\ln K_1$ measurements. The gas has been equilibrated at 1000 °C for about 5 h. We use the calculated value of $\ln K_1 = -26$ ppm at that temperature (see Table 2) to determine A_{ref} in Eq. (10). The uncer-

Temperature T (K)	$-(\ln K_1)/10^{-6}$				
	WSE2004[a 22],	CL2012[36]	WM2014[33]	CBRZ2014[54]	This work
100	4830				4850
200	1827			1842	1836
273.15	1112				1122
300	954	951	960 (9)	968	959
400	566		570 (9)		570
500	358		357 (7)		359
600	235		232 (5)		235
1000	59			51	56
1273.15	28				26
1500	17				15
2000	7				8

Table 2. Temperature dependence of the isotope equilibrium constant K_1. Different theories are employed: BMU approach using harmonic frequencies for application of the Teller-Redlich[28] rule and anharmonic correction to the ZPEs – WSE2004[22]. The same approach using harmonic frequencies from another level of theory – CL2012[36]. Path-Integral Monte Carlo (PIMC) evaluation of partition sums – WM2014[33]. Approximate direct sum partition functions from a refined potential surface – CBRZ2014[54]. Direct sum calculation of partition functions (this work) using state energies from new spectroscopic data generated from experimentally refined ab initio calculations[34]. [a]Values at temperatures other than 200, 300 and 1000 K were recalculated from molecular constants in Table 3 of Wang *et al.*[22].

tainty of this calibration is very small: different calculations at 1000 K are given in the literature[22,33,36] and our calculation based on partition functions evaluated as direct sums of energy levels provided by ab initio calculations that were refined by spectroscopic measurements[34], indicate that the error at that temperature is about 5 ppm. This deviates by only 2 ppm from the BMU method using the molecular constants of Wang *et al.*[22]. If we assume that the relative uncertainty remains the same, the systematic bias of the calibration should only be about 2 to 3 ppm at 1000 °C. Calculated room temperature (300 K) values of ln (K_1) show a larger spread between −951 and −968 ppm, giving an order of ±10 ppm agreement (see Table 2). This uncertainty span is significantly larger than the spread in the high temperature values, rendering high temperature measurement preferable for calibration. As does the temperature gradient, which is 82 times smaller than the room temperature gradient of $d \ln K_1/dT = 5.7$ ppm/K and makes the high temperature calibration less sensitive to instabilities in the temperature than its room temperature counterpart. This first calibration led us assign a value of $\ln K_{1,ref} = -(954 \pm 20)$ ppm to our room temperature reference gas (lab grade purity N4.8 from Air Liquide, $\delta^{13}C_{VPDB} = -(40.0 \pm 0.3)$‰, $\delta^{18}O_{VPDB-CO_2} = -(27.3 \pm 0.3)$‰). If not noted otherwise, we indicate measurement uncertainties as combined standard uncertainties at the 68% level of confidence.

In the second step, individual samples are measured by alternating acquisition sequences of sample and working gas. Each sequence starts by filling the spectrometer with the working reference gas and acquiring spectra for about 30 s with 1 s integration time. Then fast (~2 min) removal of the working reference occurs and the sample gas is analysed following the same acquisition procedure. Pressures of sample and reference gases are matched to agree within 0.01%. For repeated analysis, the sample is recovered using cryogenic trapping for about 5 minutes. At the end of the evacuation period the optical base line is determined. These repeated sample-reference comparisons, where Eq. (10) is applied each time, allow to take into account slow instrumental drifts that may have an impact on the determination of ln Σ.

Results and Discussion

CO_2 thermometry with $^{13}C^{16}O^{18}O$ and case application. The newly developed laser instrument has first been employed to demonstrate its capacity as CO_2 isotopologue thermometer using ln K_1 as directly observable temperature proxy. Four different samples of equilibrated CO_2 have been prepared, with equilibration temperatures at 1 °C, 21 °C, 131 °C, and 1000 °C. For measurements at 1000 °C, pure CO_2 gas was filled into quartz vials and kept in a lab oven for about 5 h. For the lower temperatures, droplets of liquid water were added to facilitate isotope exchange between isotopologues of CO_2. At 1 °C equilibration times were about one month, and they were about a week for the intermediate temperature at 131 °C. Figure 4 shows the results of the measurements in comparison to the theoretically calculated curve. As a reference we use our evaluations of K_1 from partition functions determined as direct sums and from the BMU method with harmonic frequencies and ZPE values given by Wang *et al.*[22] (see Table 2). The maximum deviation of 59 ppm between either of the theoretical calculations in Fig. 4 and the measurements has been observed at 274 K. It is within twice the combined standard uncertainty (61 ppm) of the laser spectroscopic measurements at that temperature. At room temperature or above, the observed agreement is well within one standard uncertainty, which is 25 and 33 ppm, respectively.

Clumped isotope thermometry of gas phase CO_2 originating from hydrothermal systems might provide a new and unique tracer for hydrothermal reservoir temperatures. The application is particularly relevant for studying the feasibility of the construction of hydrothermal power plants and estimating the associated risks, because the isotope thermometer may provide additional information on the related geological system and involved aquifers.

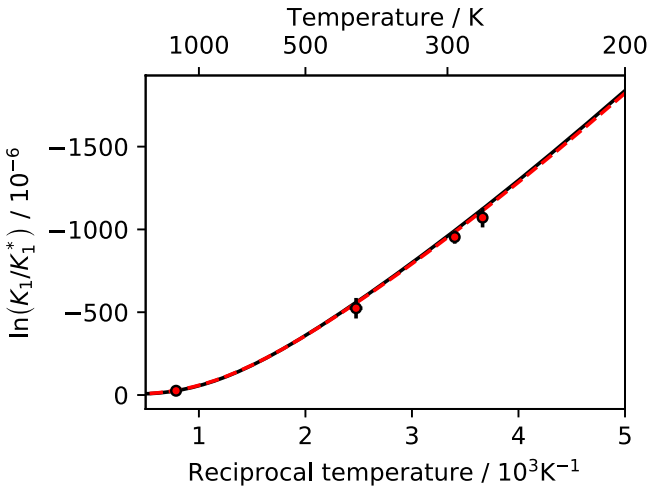

Figure 4. Measurement of the $^{12}C^{16}O_2 + {}^{13}C^{16}O^{18}O$ equilibrium constant over the 274 to 1273 K (1 to 1000 °C) temperature range. ln (K_1) is determined directly for samples of different isotopic composition that were equilibrated in quartz ($T > 1000$ K) or in pyrex tubes to which drops of liquid water were added ($T = 274$, 294 and 404 K). Data are given with combined standard uncertainties that include the uncertainty of the calibration procedure based on the working gas measurement. Solid and dashed lines indicate two different theoretical temperature dependencies (see text and caption Fig. 3 for more details). The high temperature value (practically error free) has been used to determine the isotopic composition of the room temperature working gas, with respect to which values at 274, 294 and 404 K have been determined.

For this case study we compare tuneable laser direct absorption spectroscopy (TLDAS) and IRMS measurements of the $^{13}C^{16}O^{18}O$ isotopologue in a case study of natural carbon dioxide extracted from an operating hydrothermal power plant (Soultz) and two shallow wells (Landgrafenbrunnen and Stahlbrunnen), all located in the Upper Rhine Valley. The geothermal reservoir in Soultz (Alsace, France) has a temperature of about 200 °C at a depth of 5000 m[37]. During power plant operation, the water cools down to ~150 °C at the surface. Carbon dioxide for the analysis has been sampled from a separate sampling line, where the water has been rapidly cooled down to 38.5 °C. The mass spectrometric and laser measurements show clumped isotope temperatures between 92 and 108 °C and the two methods agree well within the respective uncertainties of 8 °C for the mass spectrometer determinations and 11 °C for the laser measurements (Fig. 5). Stahlbrunnen and Landgrafenbrunnen are two hydrothermal wells in Bad Homburg, Germany. The CO_2 from the first one has been sampled directly from the well in the gas phase, whereas sampling of the carbon dioxide dissolved in water has been performed for the latter. The preparation of the gas samples for laser spectroscopic analysis follows a simplified procedure. It involves cryogenic separation from water and removal of non-condensable species through vacuum pumping. Compared to preparation for IRMS analysis, which requires additional cleaning by passage through a Porapak column[38], the total preparation time is reduced by a factor of two. Laser spectroscopy and IRMS analysis of Landgrafenbrunnen CO_2 apparent equilibrium temperatures show values of (10 ± 4) °C and (15 ± 6) °C, respectively, which is in good agreement with the temperature of the well's water, $T_w = 13.5$ °C. A slight deviation from the expected water-CO_2 equilibrium towards higher temperature has been observed for Stahlbrunnen, $T_w = 12.4$ °C versus $T_{IRMS} = (20 \pm 5)$ °C and $T_{TLDAS} = (28 \pm 7)$ °C. The interpretation of eventual discrepancies between measured apparent equilibration temperatures and parent water temperatures requires further investigation and is beyond the scope of this paper.

Future developments. The standard uncertainty of the laser measurements in the 50 ppm range is obtained with samples of about 100 µmol and about 10 sample reference comparisons, which take between 1.5 and 2 h. This is still slightly larger than what can be obtained by mass spectrometry. However, this type of optical measurements is still in its infancy and is expected to improve soon. Already, our 0.8 L Herriott cell can be replaced with a very compact 40 to 140 mL multi-pass cell[39,40] that provides a similar absorption length. Such small volumes imply reduced sample sizes on the order of 10 µmol or below and lead to faster evacuation times due to much simpler geometry without dead volumes. This shortens the time lapse between sample and reference measurement, thus limiting the impact of instrument drift and reducing the overall measurement uncertainty. We further anticipate that the introduction of an automated pressure balance system will allow for more reproducible conditions that further improve the measurement uncertainty.

It is also worth noting that optical measurements in the ν_3 fundamental region of CO_2 around 4.4 µm are not exclusively limited to the detection of the $^{13}C^{16}O^{18}O$ clumped isotopologue. Figure 1 already shows that $^{13}C^{16}O^{17}O$ can be measured as well. Inspection of spectral data[41,42] further indicates that the $P(12)e$ transition at 2305.365327 cm^{-1} provides a well isolated absorption line of $^{12}C^{18}O_2$. Its reported line strength ($S = 1.11 \cdot 10^{-23}$ cm molecule^{-1}) is similar to the intensities of $^{12}C^{16}O^{17}O$ and $^{13}C^{16}O_2$ used in this work (Fig. 1) and $^{12}C^{18}O_2$ should thus well be amenable to quantitative analysis. Given a suitable laser source, the isotopologue can be detected simultaneously with $^{12}C^{16}O_2$, $^{13}C^{16}O_2$, $^{12}C^{16}O^{18}O$ and $^{13}C^{16}O^{18}O$ and its measurement would provide a second and independent thermometer via the homogeneous

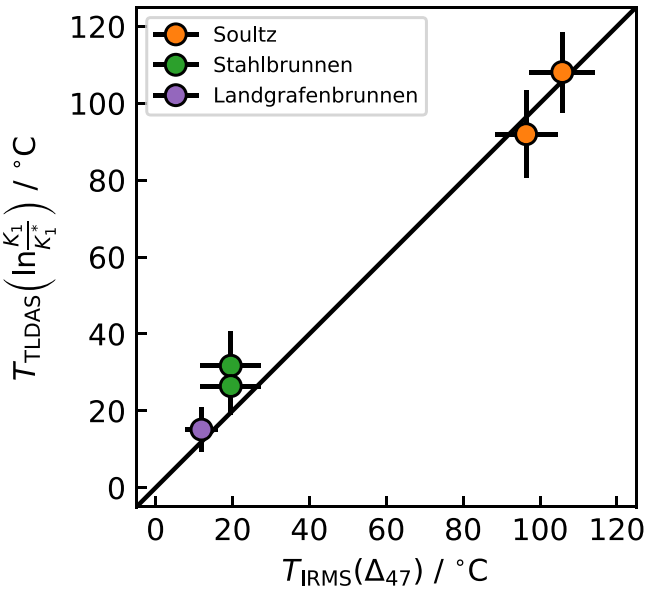

Figure 5. Comparison of optical (y-axis) and mass spectrometer (x-axis) measurements using natural samples from three sources in Germany and France. Two low temperature sources Landgrafenbrunnen (water temperature $T_w = 13.5\,°C$) and Stahlbrunnen (water temperature $T_w = 12.4\,°C$) are situated in Bad Homburg (50°13′26″ N, 8′37′21″ W) and are compared to a thermal source (sampling water temperature $T_w = 38.5\,°C$) in Soultz (47°53′12″ N, 7°13′47″ W), France. Note that both clumped isotope equilibrium methods are consistent in magnitude and relative to each other. Uncertainties as well as combined preparation plus analysis times are similar for both, mass spectrometer and laser measurements.

$$^{12}C^{18}O_2 + {}^{12}C^{16}O_2 \rightleftharpoons 2\,{}^{12}C^{16}O^{18}O \tag{R2}$$

exchange reaction, whose equilibrium constant has a temperature coefficient ($d\ \ln(K_2/4)/dT = 3.5$ ppm/K) of the same magnitude than K_1 at 300 K (see Fig. 3). The advantage of using this clumped CO_2 thermometer along with $^{13}C^{16}O^{18}O$ thermometry is its independence from ^{13}C. The presence of kinetic fractionation effects that possibly compromise equilibrium thermometer readings would thus likely be different in the ^{13}C containing and in the ^{13}C free clumped isotope systems[43–46]. These effects could thus potentially be identified and corrected for. Therefore, optical measurements could provide an entirely new level of temperature information in the future. As an aside, we mention that clumped isotopes are often discussed in terms of bond ordering[4,47], *i.e.* whether two rare isotopes form a common bond, such as ^{13}C-^{18}O in $^{13}C^{16}O^{18}O$. Reaction R2 is an example of indirect isotope clumping, where the two rare isotopes do not share the same bond[1]. In larger molecules, such as propane, ethane etc. this will be the predominant clumping mechanism. By definition, statistical combination of two different isotopic reservoirs leads to position-independent (anti-)clumping[48,49]. The similar magnitude of isotope fractionation in both reactions R2 and R1 (Fig. 3) demonstrates that thermodynamic clumping effects should also be considered as concentrating two (or more) rare isotopes in the same molecule, leading to a molecular configuration which is thermodynamically more stable than when these isotopes are redistributed over two (or more) different molecules – irrespective whether these isotopes share the same chemical bond or not.

Finally, the direct measurement of the equilibrium constant of an homogeneous exchange reaction at ppm accuracy may provide an interesting benchmark for molecular quantum calculations and potential energy surfaces. At low temperatures, different models are particularly sensitive to ZPE differences ($\Delta\nu_0$ and the energies of the lowest states (see Eqs (8) or (9)). At 300 K the ZPE difference factor $\exp(-c_2\Delta\nu_0/T)$ deviates from unity by 5 parts in 10^6 if $\Delta\nu_0 = 0.001\ cm^{-1}$. This implies that an uncertainty of a few ppm – a range that will be amenable to measurements in the near future – is sufficient to determine ZPE differences at the $0.001\ cm^{-1}$ uncertainty level, irrespective whether the ZPE differences are large, as in the case of the $H_2 + D_2 \rightleftharpoons 2$ HD reaction where $\Delta\nu_0 = 54.867\ cm^{-1}$ [50,51], or small – as in reaction R1, where calculated values[22,33,34] range from 0.433 to 0.435 cm^{-1}.

Summary and Conclusion

We provide the first optical measurement of multiply-substituted isotopologues of CO_2 at the accuracy level of better than 100 ppm. New advances in laser absorption spectroscopy, such as evidenced by the recent measurement of $^{12}C^{16}O^{17}O$ at the precision level of 10 ppm within a time frame of 10 min[52], indicate that laser instruments will favourably compete with mass spectrometer technology very soon. The comparatively high selectivity of laser-based instruments and their large potential of assessing new tracers, such as $^{12}C^{18}O_2$ for the homogeneous isotope exchange with $^{12}C^{16}O_2$, will open up new horizons in clumped isotope science and thermometry. The most important advantage of the technology is that the temperature can be obtained easily and directly via an unambiguous measurement of the equilibrium constant of the isotope exchange reaction. The optical CO_2

isotopologue thermometer is a strong example showcasing the full potential for this and other molecules in the future. We have shown how the technology can be used for the thermometry of gaseous CO_2 and that new areas related to molecular chemistry and physics are opened up for clumped isotope research. The relatively low cost and size factors of the technology will be additional parameters for developing and easing the spread of this exciting frontier science technology to more laboratories and technological applications.

References

1. Eiler, J. M. "Clumped-isotope" geochemistry–the study of naturally-occurring, multiply-substituted isotopologues. *Earth Planet Sci. Lett.* **262**, 309–327 (2007).
2. Eiler, J. M. *et al*. Frontiers of stable isotope geoscience. *Chem. Geol.* **372**, 119–143 (2014).
3. Tsuji, K., Teshima, H., Sasada, H. & Yoshida, N. Spectroscopic isotope ratio measurement of doublysubstituted methane. *Spectrochim. Acta A* **98**, 43–46 (2012).
4. Young, E. D. *et al*. The relative abundances of resolved $^{12}CH_2D_2$ and $^{13}CH_3D$ and mechanisms controlling isotopic bond ordering in abiotic and biotic methane gases. *Geochim. Cosmochim. Acta* **203**, 235–264 (2017).
5. Ono, S. *et al*. Measurement of a doubly substituted methane isotopologue, $^{13}CH_3D$, by tunable infrared laser direct absorption spectroscopy. *Anal. Chem.* **86**, 6487–6494 (2014).
6. Coplen, T. B. *et al*. Isotope-abundance variations of selected elements - (IUPAC technical report). *Pure Appl. Chem.* **74**, 1987–2017 (2002).
7. Brenninkmeijer, C. A. M. & Röckmann, T. A rapid method for the preparation of O_2 from CO_2 for mass spectrometric measurement of $^{17}O/^{16}O$ ratios. *Rapid Commun. Mass Spectrom.* **12**, 479–483 (1998).
8. Barkan, E. & Luz, B. High-precision measurements of $^{17}O/^{16}O$ and $^{18}O/^{16}O$ ratios in CO_2. *Rapid Commun. Mass Spectrom.* **26**, 2733–2738 (2012).
9. Assonov, S. S. & Brenninkmeijer, C. A. M. A new method to determine the ^{17}O isotopic abundance in CO_2 using oxygen isotope exchange with a solid oxide. *Rapid Commun. Mass Spectrom.* **15**, 2426–2437 (2001).
10. Huntington, K. W. *et al*. Methods and limitations of 'clumped' CO_2 isotope (Δ_{47}) analysis by gas-source isotope ratio mass spectrometry. *J. Mass. Spec.* **44**, 1318–1329 (2009).
11. Dennis, K. J., Affek, H. P., Passey, B. H., Schrag, D. P. & Eiler, J. M. Defining an absolute reference frame for 'clumped' isotope studies of CO_2. *Geochim. Cosmochim. Acta* **75**, 7117–7131 (2011).
12. Wacker, U., Fiebig, J. & Schoene, B. R. Clumped isotope analysis of carbonates: comparison of two different acid digestion techniques. *Rapid Commun. Mass Spectrom.* **27**, 1631–1642 (2013).
13. Kluge, T., John, C. M., Jourdan, A.-L., Davis, S. & Crawshaw, J. Laboratory calibration of the calcium carbonate clumped isotope thermometer in the 25–250 °C temperature range. *Geochim. Cosmochim. Acta* **157**, 213–227 (2015).
14. Young, E. D., Rumble, D. III., Freedman, P. & Mills, M. A large-radius high-mass-resolution multiple-collector isotope ratio mass spectrometer for analysis of rare isotopologues of O_2, N_2, CH_4 and other gases. *Int. J. Mass Spectrom.* **401**, 1–10 (2016).
15. He, B., Olack, G. A. & Colman, A. S. Pressure baseline correction and high-precision CO_2 clumped-isotope (Δ_{47}) measurements in bellows and micro-volume modes. *Rapid Commun. Mass Spectrom.* **26**, 2837–2853 (2012).
16. Laskar, A. H., Mahata, S. & Liang, M.-C. Identification of anthropogenic CO_2 using triple oxygen and clumped isotopes. *Environ. Sci. Technol.* **50**, 11806–11814 (2016).
17. Prokhorov, I. *Optical carbon dioxide isotopologue thermometry*. Ph.D. thesis, Heidelberg University (2018).
18. Gordon, I. *et al*. The HITRAN2016 molecular spectroscopic database. *J. Spectrosc. Radiat. Transf.* **203**, 3–69 (2017).
19. Minissale, M., Zanon-Willette, T., Prokhorov, I., Elandaloussi, H. & Janssen, C. Non-linear frequency-sweep correction of tunable electromagnetic sources. *IEEE Trans. Ultrason. Ferroelectr. Freq. Control* **65**, 1487–1491 (2018).
20. Rautian, S. G. & Sobel'man, I. I. The effect of collisions on the Doppler broadening of spectral lines. *Usp. Fiz. Nauk.* **90**, 209–236 [Sov. Phys. Usp. 9, 701 (1967)] (1966).
21. Guinet, M., Mondelain, D., Janssen, C. & Camy-Peyret, C. Laser spectroscopic study of ozone in the 100 ← 000 band for the SWIFT instrument. *J. Quant. Spectrosc. Radiat. Transf.* **111**, 961–972 (2010).
22. Kerstel, E. Isotope ratio infrared spectrometry. In de Groot, P. (ed.) *Handbook of Stable Isotope Analytical Techniques*, chap. **34**, 759–792 (Elsevier, 2004).
23. Brenninkmeijer, C. A. M. *et al*. Isotope effects in the chemistry of atmospheric trace compounds. *Chem. Rev.* **103**, 5125–5161 (2003).
24. Wang, Z., Schauble, E. A. & Eiler, J. M. Equilibrium thermodynamics of multiply substituted isotopologues of molecular gases. *Geochim. Cosmochim. Acta* **68**, 4779–4797 (2004).
25. Mauersberger, K., Morton, J., Schueler, B., Stehr, J. & Anderson, S. M. Multi-isotope study of ozone: implications for the heavy ozone anomaly. *Geophys. Res. Lett.* **20**, 1031–1034 (1993).
26. Mayer, J. E. & Goeppert-Mayer, M. *Statistical Mechanics* (John Wiley & Sons, Inc., New York, London, Sydney, 1940).
27. Huang, X., Schwenke, D. W., Freedman, R. S. & Lee, T. J. Ames-2016 line lists for 13 isotopologues of CO_2: Updates, consistency, and remaining issues. *J. Quant. Spectrosc. Radiat. Transf.* **203**, 224–241 (2017).
28. Daëron, M., Blamart, D., Peral, M. & Affek, H. P. Absolute isotopic abundance ratios and the accuracy of Δ_{47} measurements. *Chem. Geol.* **442**, 83–96 (2016).
29. Bigeleisen, J. & Goeppert Mayer, M. Calculation of equilibrium constants for isotopic exchange reactions. *J. Chem. Phys.* **15**, 261–267 (1947).
30. Urey, H. C. & Greiff, L. J. Isotopic exchange equilibria. *J. Am. Chem. Soc.* **57**, 321–327 (1935).
31. Redlich, O. A general relationship between the oscillation frequency of isotropic molecules - (with remarks on the calculation of harmonious force constants). *Z. Physik. Chem. B* **28**, 371–382 (1935).
32. Urey, H. C. The thermodynamic properties of isotopic substances. *J. Chem. Soc.* 562–581 (1947).
33. Richet, P., Bottinga, Y. & Javoy, M. Review of hydrogen, carbon, nitrogen, oxygen, sulfur, and chlorine stable isotope fractionation among gaseous molecules. *Ann. Rev. Earth Planet. Sci.* **5**, 65–110 (1977).
34. Liu, Q., Tossell, J. A. & Liu, Y. On the proper use of the Bigeleisen–Mayer equation and corrections to it in the calculation of isotopic fractionation equilibrium constants. *Geochim. Cosmochim. Acta* **74**, 6965–6983 (2010).
35. Zimmermann, T. & Vaníček, J. Path integral evaluation of equilibrium isotope effects. *J. Chem. Phys.* **131**, 024111–14 (2009).
36. Webb, M. A. & Miller, T. F. III. Position-specific and clumped stable isotope studies: Comparison of the Urey and path-integral approaches for carbon dioxide, nitrous oxide, methane, and propane. *J. Phys. Chem. A* **118**, 467–474 (2014).
37. Gamache, R. R. *et al*. Total internal partition sums for 166 isotopologues of 51 molecules important in planetary atmospheres: Application to HITRAN2016 and beyond. *J. Quant. Spectrosc. Radiat. Transf.* **203**, 70–87 (2017).
38. Cao, X. & Liu, Y. Theoretical estimation of the equilibrium distribution of clumped isotopes in nature. *Geochim. Cosmochim. Acta* **77**, 292–303 (2012).
39. Cerezo, J., Bastida, A., Requena, A. & Zúñiga, J. Rovibrational energies, partition functions and equilibrium fractionation of the CO_2 isotopologues. *J. Quant. Spectrosc. Radiat. Transf.* **147**, 233–251 (2014).
40. Sanjuan, B. *et al*. Major geochemical characteristics of geothermal brines from the Upper Rhine Graben granitic basement with constraints on temperature and circulation. *Chem. Geol.* **428**, 27–47 (2016).

41. Petersen, S. V., Winkelstern, I. Z., Lohmann, K. C. & Meyer, K. W. The effects of Porapak trap temperature on $\delta^{18}O$, $\delta^{13}C$, and Δ_{47} values in preparing samples for clumped isotope analysis. *Rapid Commun. Mass Spectrom.* **30**, 199–208 (2016).
42. Tuzson, B., Mangold, M., Looser, H., Manninen, A. & Emmenegger, L. Compact multipass optical cell for laser spectroscopy. *Opt. Lett.* **38**, 257–259 (2013).
43. Graf, M., Emmenegger, L. & Tuzson, B. Compact, circular, and optically stable multipass cell for mobile laser absorption spectroscopy. *Opt. Lett.* **43**, 2434–2437 (2018).
44. Zak, E. J. *et al.* Room temperature linelists for CO_2 symmetric isotopologues with ab initio computed intensities. *J. Quant. Spectrosc. Radiat. Transf.* **189**, 265–281 (2017).
45. Zeebe, R. E. Kinetic fractionation of carbon and oxygen isotopes during hydration of carbon dioxide. *Geochim. Cosmochim. Acta* **139**, 540–552 (2014).
46. Sade, Z. & Halevy, I. New constraints on kinetic isotope effects during CO_2(aq) hydration and hydroxylation: Revisiting theoretical and experimental data. *Geochim. Cosmochim. Acta* **214**, 246–265 (2017).
47. Guo, W. *Carbonate clumped isotope thermometry: application to carbonaceous chondrites and* effects *of kinetic isotope fractionation*. Ph.D. thesis, California Institute of Technology (2009).
48. Watkins, J. & Hunt, J. A process-based model for non-equilibrium clumped isotope effects in carbonates. *Earth Planet Sci. Lett.* **432**, 152–165 (2015).
49. Tripati, A. K. *et al.* Beyond temperature: Clumped isotope signatures in dissolved inorganic carbon species and the influence of solution chemistry on carbonate mineral composition. *Geochim. Cosmochim. Acta* **166**, 344–371 (2015).
50. Röckmann, T., Popa, M. E., Krol, M. C. & Hofmann, M. E. G. Statistical clumped isotope signatures. *Sci. Rep.* **6**, 31947 (2016).
51. Yeung, L. Y. Combinatorial effects on clumped isotopes and their significance in biogeochemistry. *Geochim. Cosmochim. Acta* **172**, 22–38 (2016).
52. Komasa, J. *et al.* Quantum electrodynamics effects in rovibrational spectra of molecular hydrogen. *J. Chem. Theory Comput.* **7**, 3105–3115 (2011).
53. Popa, M. E., Paul, D., Janssen, C. & Röckmann, T. H_2 clumped isotope measurements at natural isotopic abundances. *Rapid Commun. Mass Spectrom.* **33**, 239–251 (2018).
54. Stoltmann, T., Casado, M., Daëron, M., Landais, A. & Kassi, S. Direct, precise measurements of isotopologue abundance ratios in CO_2 using molecular absorption spectroscopy: Application to $\Delta^{17}O$. *Anal. Chem.* **89**, 10129–10132 (2017).

Acknowledgements

I.P. and T.K. acknowledge funding from the Heidelberg Graduate School of Fundamental Physics (HGSFP). We acknowledge the technical help of the 'physics of environmental archives' team to maintain the IRMS instrument that was funded through the grant DFG-INST 35/1270-1. We thank Thomas Neumann, Elisabeth Eiche and Michael Kraml for support in selecting and sampling of hydrothermal wells. We are grateful for assistance by Maximilian Kalb and Andreas Weise in sampling CO_2 at Soultz. We also thank Nicolas Cuenot for enabling access to the hydrothermal plant at Soultz and for technical support. C.J. would like to acknowledge Norbert Frank for invitation to a visiting professorship at IUP Heidelberg during this work.

Author Contributions

I.P. and C.J. planned the work, I.P. set up the instrument, made the laser measurements and performed the analysis. C.J. contributed to the instrumental set up. I.P. and T.K. collected geothermal CO_2 samples. T.K. performed the IRMS analysis. All authors wrote and reviewed the manuscript.

Additional Information

Competing Interests: The authors declare no competing interests.

Publisher's note: Springer Nature remains neutral with regard to jurisdictional claims in published maps and institutional affiliations.